

## Exciton-phonon interactions and exciton dephasing in semiconductor quantum-well heterostructures

I. V. Bondarev, S. A. Maksimenko, and G. Ya. Slepyan

*The Institute for Nuclear Problems, The Belarusian State University, Bobruiskaya Street 11, 220050 Minsk, Belarus*

I. L. Krestnikov\* and A. Hoffmann

*Institut für Festkörperphysik, Technische Universität Berlin, Hardenbergstrasse 36, 10623 Berlin, Germany*

(Received 9 June 2003; published 29 August 2003)

We have investigated exciton-phonon coupling and related exciton dephasing processes in monolayer semiconductor heterostructures with localized quasi two-dimensional (2D) excitonic states. The calculated lateral size dependence of low-temperature Huang-Rhys factors indicates the enhancement of exciton-phonon coupling with decreasing the lateral size of the quasi-2D exciton localization area. This entails the increase of exciton dephasing. At low temperatures, the exciton absorption line exhibits an essentially non-Lorentzian asymmetric shape with the asymmetry increasing with the decrease of temperature and the lateral size of the quasi-2D exciton localization area.

DOI: 10.1103/PhysRevB.68.073310

PACS number(s): 78.67.-n, 68.65.-k, 71.35.-y, 72.10.Di

Quasimonolayer semiconductor heterostructures have attracted considerable attention of experimentalists due to their unique physical properties and their applications in modern nanoelectronics as various light emitting devices and logic devices for quantum information processing. In such systems, the fluctuation of the quantum-well (QW) thickness produces the fluctuation of the translational energy of quasi-two-dimensional (2D) excitons, making them localize at energetically local minimum sites in islandlike structures of several tens of nanometers in diameter.<sup>1,2</sup> These localized excitonic states can be regarded as weakly confined quantum dot (QD) like states. One dimension of the confinement is defined by the QW width (typically from one to several monolayers), while the other two lateral dimensions are defined by the effective size of the island. Recent experiments have demonstrated a key role of exciton-phonon interactions in such systems for both III-V and II-VI heterostructures.<sup>3,4</sup> In particular, acoustic phonons were shown to be responsible for the non-Lorentzian behavior of the exciton emission line with increasing temperature,<sup>3</sup> whereas the interactions with optical phonons were demonstrated to lead to the formation of strong-coupling polarons.<sup>4</sup>

We analyze exciton-phonon coupling and related exciton dephasing processes in the systems above. This is extremely important for technological applications since dephasing due to the exciton-phonon interactions is responsible for homogeneous broadening a QD optical absorption line that cannot be eliminated by better sample fabrication. All exciton-phonon interaction mechanisms have been considered. They are the polar optical (Froehlich) interaction, the optical deformation potential, the acoustic deformation potential, and the acoustic piezoelectric interaction. We calculate low-temperature Huang-Rhys factors and optical absorption line shapes and demonstrate the increase of the formers and non-Lorentzian behavior of the latters with decreasing the lateral size of the quasi-2D exciton localization area. We emphasize that, contrary to QD nanocrystallites where the adiabatic Huang-Rhys concept is either inapplicable at all due to the strong inharmonicity<sup>5</sup> or sometimes applicable in the strong

confinement regime,<sup>6</sup> we deal with the situation where the quasi-2D exciton is weakly confined in the lateral plane of a *thick* planar superlattice of two semiconductors with similar dielectric and elastic properties and different band gaps. Typical examples are InAs-GaAs, CdTe-ZnTe, InGaAsN, etc.<sup>1-4</sup>

In the case of QW heterostructures, the electron and hole of the exciton are well confined within the layer since the band-gap discontinuity is quite large, especially for III-V heterostructures. On the other hand, dielectric and lattice properties of group III (II) and group V (VI) semiconductors (dielectric permittivities, lattice constants, elastic moduli) are in close proximity in their values.<sup>7</sup> Therefore, we model our system by the localized quasi-2D 1S-exciton interacting with bulklike phonon modes in QW with infinite potential barriers. We describe such an excitonic state by the quasi-2D wave function

$$|\mathbf{R}_0\rangle = \nu_0 \sum_{\mathbf{r}_e, \mathbf{r}_h} f(\mathbf{R}_\parallel - \mathbf{R}_0) F_{1S}(\mathbf{r}_e) - \mathbf{r}_h \parallel, z_e, z_h; \alpha, \beta) a_{c\mathbf{r}_e}^+ a_{v\mathbf{r}_h} |0\rangle \quad (1)$$

with the in-plane Gaussian distribution  $f(\mathbf{R}_\parallel - \mathbf{R}_0) = \exp[-(\mathbf{R}_\parallel - \mathbf{R}_0)^2/2\xi^2]/\xi\sqrt{\pi}$  of the exciton center-of-mass motion around the localization center at the point  $\mathbf{R}_0$  and the exciton envelope function  $F_{1S}$  of an exponential form with two variational parameters  $\alpha$  and  $\beta$ .<sup>8</sup> The operator  $a_{c\mathbf{r}_e}^+$  creates the electron in the conduction band at the point  $\mathbf{r}_e$  and the operator  $a_{v\mathbf{r}_h}$  annihilates the electron, creating the hole in the valence band at the point  $\mathbf{r}_h$ ;  $|0\rangle$  is the ground state of the system,  $\nu_0$  is the volume of the unit cell,  $\mathbf{R}_\parallel = \mu_e \mathbf{r}_e \parallel + \mu_h \mathbf{r}_h \parallel$  is the in-plane excitonic center-of-mass coordinate with  $\mu_{e,h} = m_{e,h}/(m_e + m_h)$ , where  $m_e$  ( $m_h$ ) is the electron (hole) effective mass. The parameter  $\xi$  in  $f(\mathbf{R}_\parallel - \mathbf{R}_0)$  is the excitonic localization length. The quantity  $R = 2\sqrt{2} \ln 2 \xi$  may be considered as a typical lateral size of the localization

area of the excitonic center of mass or, in other words, as a typical lateral size of QD.

The total Hamiltonian of the system is of the form

$$\hat{H} = \hat{H}_e + \hat{H}_{ph} + \hat{H}_{int} = E_0 B^\dagger B + \sum_{\mathbf{q}, l} \hbar \omega_{\mathbf{q}l} (b_{\mathbf{q}l}^\dagger b_{\mathbf{q}l} + 1/2) + B^\dagger B \sum_{\mathbf{q}, l} M_{\mathbf{q}l} (b_{\mathbf{q}l}^\dagger + b_{-\mathbf{q}l}), \quad (2)$$

where  $B^\dagger$  ( $B$ ) are the creation (annihilation) operators of the localized quasi-2D exciton with the energy  $E_0$ ,  $b_{\mathbf{q}l}^\dagger$  ( $b_{\mathbf{q}l}$ ) are those for the phonon of the branch  $l$  with the momentum  $\mathbf{q}$  and the energy  $\hbar \omega_{\mathbf{q}l}$ . The first two terms of the Hamiltonian describe the exciton and phonon subsystems. The third one is their interaction represented by the diagonal interaction matrix element

$$M_{\mathbf{q}l} = \langle \mathbf{R}_0 | w_e(\mathbf{q}, l) e^{i\mathbf{q} \cdot \mathbf{r}_e} - w_h(\mathbf{q}, l) e^{i\mathbf{q} \cdot \mathbf{r}_h} | \mathbf{R}_0 \rangle, \quad (3)$$

where  $w_{e,h}(\mathbf{q}, l)$  depends on the type of the exciton-phonon interaction (enumerated by  $l$ ). Specifically,  $w_{e,h} = -(e/q) \sqrt{2\pi\hbar\omega_0(1/\epsilon_\infty - 1/\epsilon_0)/L^3}$  for the polar optical interaction,  $w_{e,h} = -D_o^{(e,h)} \sqrt{\hbar/2\omega_0 L^3 \rho}$  for the optical deformation potential,  $w_{e,h} = -E_d^{(e,h)} q \sqrt{\hbar/2\omega_{\mathbf{q}LA} L^3 \rho}$  for the acoustic deformation potential interaction, and  $w_{e,h} = -(8\pi e e_{14}/\epsilon_0 q^2) \sqrt{\hbar/2\omega_{\mathbf{q}LA(TA)} L^3 \rho} (e_x q_y q_z + e_y q_z q_x + e_z q_x q_y)$  for the acoustic piezoelectric interaction, where  $L$ ,  $\rho$ , and  $\epsilon_{\infty,0}$  are the linear size, density, and dynamic (static) dielectric permittivity of the quantization area, respectively,  $e$  is the electron charge,  $D_o^{(e,h)}$  and  $E_d^{(e,h)}$  are the optical and acoustic deformation potential coupling constants,  $e_{14}$  is the electromechanical piezoelectric constant of zinc-blende-type crystals,  $\omega_0$  is the frequency of optical vibrations, and  $\omega_{\mathbf{q}LA(TA)} = u_{LA(TA)} q$  is the frequency of LA (TA) acoustic vibrations with the velocity  $u_{LA(TA)}$  and the unit polarization vectors  $\mathbf{e}(LA) = (q_x, q_y, q_z)/q$ ,  $\mathbf{e}(TA1) = (q_y, -q_x, 0)/\sqrt{q_x^2 + q_y^2}$ ,  $\mathbf{e}(TA2) = (-q_x q_z, -q_y q_z, q_x^2 + q_y^2)/q\sqrt{q_x^2 + q_y^2}$ .<sup>7,8</sup>

Hamiltonian (2) ignores the off-diagonal exciton-phonon interaction. Its role is suppressed at low temperatures, where we are interested in. Within the framework of this approximation, exciton-phonon coupling self-consistently changes the equilibrium lattice position and lowers the exciton energy by the value which, being normalized by the phonon energy, represents the dimensionless exciton-phonon coupling constant, the Huang-Rhys factor,<sup>5,6</sup>  $S_l(T) = \sum_{\mathbf{q}l} |M_{\mathbf{q}l}|^2 (2n_{\mathbf{q}l} + 1) / (\hbar \omega_{\mathbf{q}l})^2$ , where  $n_{\mathbf{q}l} = [\exp(\hbar \omega_{\mathbf{q}l} / k_B T) - 1]^{-1}$  is the phonon occupation number and  $M_{\mathbf{q}l}$  is defined by Eq. (3) with  $|\mathbf{R}_0\rangle$  given by Eq. (1). For a single monolayer (ML), this reduces to

$$S_l(T) = \sum_{\mathbf{q}l} \frac{e^{-\xi^2 \mathbf{q}^2 / 2}}{(\hbar \omega_{\mathbf{q}l})^2} (2n_{\mathbf{q}l} + 1) \left\{ \frac{w_e(\mathbf{q}l, l)}{[1 + (\mu_h q_{\parallel} / 2\alpha)^2]^{3/2}} - \frac{w_h(\mathbf{q}l, l)}{[1 + (\mu_e q_{\parallel} / 2\alpha)^2]^{3/2}} \right\}^2, \quad (4)$$

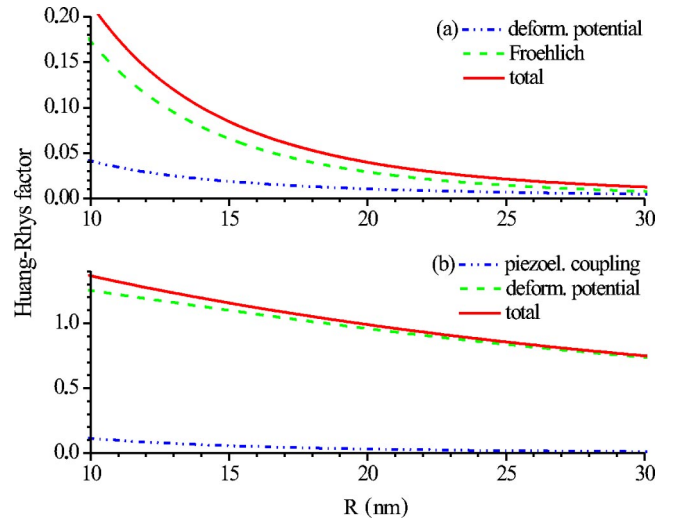


FIG. 1. (Color online) Optical (a) and acoustic (b) zero-temperature Huang-Rhys factors of localized quasi-2D excitons.

where  $\mathbf{q}_{\parallel}$  is the in-plane phonon momentum and  $w_{e,h}$  differ from those in Eq. (3) by the replacement  $L^3 \rightarrow L^2 a_0$ , with  $a_0 = \sqrt[3]{v_0}$  being the average interatomic distance in zinc-blende-type crystals.

We calculated zero-temperature Huang-Rhys factors (4) as functions of the QD lateral size using the physical parameters of GaAs.<sup>7</sup> The optical Huang-Rhys factors are represented in Fig. 1(a). Both Froehlich contribution and optical deformation potential contribution (caused by the heavy-hole interaction in a  $p$ -like valence band) increase as the QD size decreases, so that the total optical Huang-Rhys factor smoothly goes up with decreasing the QD lateral size. The Froehlich contribution dominates over that of the optical deformation potential at small sizes  $\sim 10$ – $20$  nm, where it exceeds its bulk value 0.0079 (Ref. 10) by at least one order of magnitude. The acoustic Huang-Rhys factors are shown in Fig. 1(b). Acoustic deformation potential coupling is seen to completely dominate over acoustic piezoelectric coupling. The total acoustic Huang-Rhys factor is  $\sim 1$  and gradually increases with decreasing the QD size. This indicates rather strong exciton-acoustic-phonon coupling which enhances with the reduction of the QD lateral size. Note that the range considered of the typical QD sizes totally corresponds to the weak lateral exciton confinement since the bulk exciton Bohr radius  $a_B$  in GaAs is  $\sim 10$  nm and the Bohr radius of the quasi-2D exciton is  $\sim a_B/2$ .<sup>7</sup>

Obviously, in small enough QD's the increase of exciton-phonon coupling should entail fast exciton dephasing with respective (homogeneous) broadening of the QD optical absorption line. To analyze the line shape, we start with the absorption spectrum  $I(E)$  represented in view of the Fermi golden rule as<sup>11</sup>

$$I(E) = \frac{2\pi}{\hbar} \left\langle \sum_f \left| \langle f | V_R | g \rangle \right|^2 \delta(E - E_g + E_f) \right\rangle, \quad (5)$$

where  $V_R$  is the electromagnetic interaction,  $|g\rangle$  and  $|f\rangle$  are the initial ground state and the final excited state with the energies  $E_g$  and  $E_f$ , respectively. The ground state of the

system is the lattice with a phonon bath, and the excited state is the localized quasi-2D exciton coupled with phonons. Averaging  $\langle \dots \rangle$  is taken over the phonon bath.

Equation (5) can be rewritten to give

$$I(E) = |V_R|^2 A(E),$$

with

$$A(E) = -2 \operatorname{Im} \int_{-\infty}^{\infty} G(t) e^{iEt/\hbar} dt \quad (6)$$

being the density of final states of the system [normalized by the condition  $(1/2\pi) \int_{-\infty}^{\infty} A(E) dE = 1$ ], where  $G(t) = (i\hbar)^{-1} \vartheta(t) \langle [B(t), B^+(0)] \rangle$  is the retarded Green's function of the localized quasi-2D exciton in the Heisenberg representation and  $\vartheta(t)$  is the step function. For the system described by Hamiltonian (2), there is an *exact* solution for  $G(t)$  given by<sup>9</sup>

$$G(t) = (i\hbar)^{-1} \vartheta(t) e^{-iE_0 t/\hbar - \phi(t)}, \quad (7)$$

with

$$\begin{aligned} \phi(t) = \sum_{\mathbf{q},l} \frac{|M_{\mathbf{q}l}|^2}{(\hbar \omega_{\mathbf{q}l})^2} & [-i\omega_{\mathbf{q}l}t + (n_{\mathbf{q}l} + 1)(1 - e^{-i\omega_{\mathbf{q}l}t}) \\ & + n_{\mathbf{q}l}(1 - e^{i\omega_{\mathbf{q}l}t})]. \end{aligned}$$

Thus, the low-temperature QD absorption spectrum (or emission spectrum which is just the mirror image of the absorption spectrum about the zero-phonon line) is completely determined by spectral density  $A(E)$  defined by Eqs. (6) and (7). Since Hamiltonian (2) neglects the off-diagonal exciton-phonon interaction,  $A(E)$  does not take into account the longitudinal relaxation of excitonic states (exciton level population decay) which induces exciton dephasing via *inelastic* exciton-phonon scattering, reducing the lifetime of the excitonic state and thereby broadening the exciton absorption line. However,  $A(E)$  *exactly* accounts for exciton pure dephasing caused by *elastic* virtual phonon scattering of the ground-state exciton, described by the diagonal interaction term in Eq. (2). According to Takagahara,<sup>11</sup> this is so-called ‘‘intra-exciton ground state’’ pure dephasing, which is expected to be of major importance for small enough QD's at low temperatures.

Since localized quasi-2D excitons are weakly coupled with optical phonons [Fig. 1(a)], the most of the spectral weight of the QD optical absorption line will be in the zero-optical-phonon line. Its shape will be determined by the acoustic exciton-phonon interaction governed by the acoustic deformation potential [Fig. 1(b)]. Then, neglecting the piezoelectric interaction, one has from Eqs. (6) and (7) the optical absorption line shape of the 1-ML-thick QD in the form

$$A(E) = \frac{2}{\hbar} \int_0^{\infty} e^{-C(t)} \cos \left[ (E - E_0 + \Delta) \frac{t}{\hbar} - D(t) \right] dt, \quad (8)$$

where

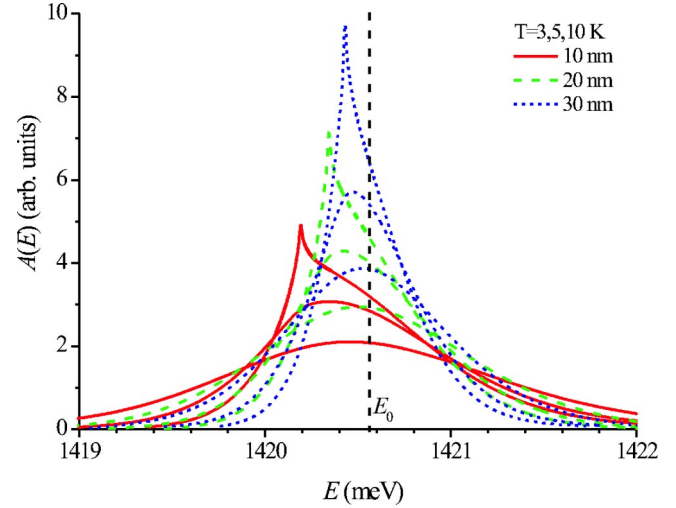


FIG. 2. (Color online) The low-temperature spectral densities at different QD sizes. Broader line corresponds to higher temperature.

$$C(t) = 2 \sum_{\mathbf{q}_{\parallel}} \frac{|M_{\mathbf{q}_{\parallel}LA}|^2}{(\hbar \omega_{\mathbf{q}_{\parallel}LA})^2} (2n_{\mathbf{q}_{\parallel}LA} + 1) \sin^2 \left( \frac{\omega_{\mathbf{q}_{\parallel}LA} t}{2} \right),$$

$$D(t) = \sum_{\mathbf{q}_{\parallel}} \frac{|M_{\mathbf{q}_{\parallel}LA}|^2}{(\hbar \omega_{\mathbf{q}_{\parallel}LA})^2} \sin(\omega_{\mathbf{q}_{\parallel}LA} t), \quad \Delta = \sum_{\mathbf{q}_{\parallel}} \frac{|M_{\mathbf{q}_{\parallel}LA}|^2}{\hbar \omega_{\mathbf{q}_{\parallel}LA}}$$

with the matrix element squared

$$|M_{\mathbf{q}_{\parallel}LA}|^2 = e^{-\xi^2 \mathbf{q}_{\parallel}^2 / 2} \left\{ \frac{w_e(\mathbf{q}_{\parallel}, LA)}{[1 + (\mu_h q_{\parallel} / 2\alpha)^2]^{3/2}} - \frac{w_h(\mathbf{q}_{\parallel}, LA)}{[1 + (\mu_e q_{\parallel} / 2\alpha)^2]^{3/2}} \right\}^2, \quad (9)$$

where  $w_{e,h}$  are those in Eq. (3) for the acoustic deformation potential with the replacement  $L^3 \rightarrow L^2 a_0$ .

The low-temperature spectral densities calculated from Eqs. (8) and (9) for GaAs QD's of different lateral sizes are shown in Fig. 2. The asymmetric non-Lorentzian behavior is clearly seen, especially at very low temperatures below 5 K where the line shape obviously cannot be described by only one parameter such as the dephasing rate. This suggests a *non-Markovian* process for virtual elastic phonon scattering of localized quasi-2D excitons. As temperature goes up, the line shape resembles the one-parametric one. However, the asymmetry still remains and decreases with increasing the QD lateral size and temperature. Figure 3 demonstrates the size and temperature dependence of the spectral density full width at half maximum (FWHM), which represents the ‘‘effective’’ exciton pure dephasing rate above 5 K.

In Fig. 4, we show the results of least-squares fitting the small- and large-QD-size spectral densities at low and elevated temperatures. The spectrum is nicely fitted by a Lorentzian function at the large size and low temperature. This indicates the *weak* quasi-2D exciton-phonon coupling regime. Decreasing the size with no temperature variation yields the asymmetric non-Lorentzian line shape representing the *intermediate* coupling regime. Further increase of

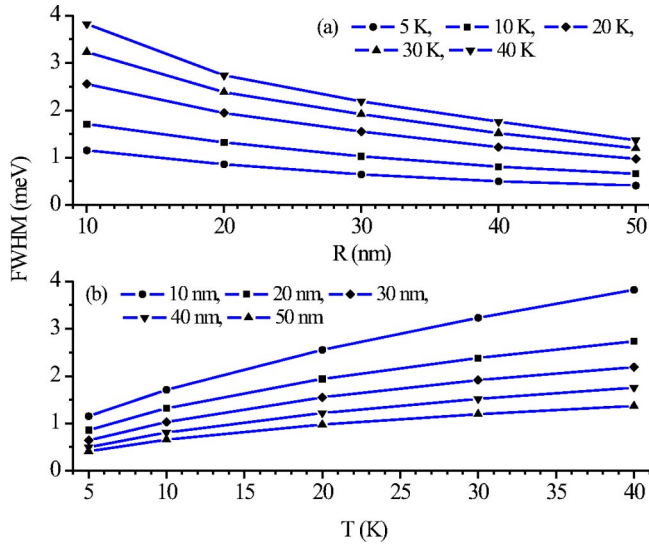


FIG. 3. (Color online) Size (a) and temperature (b) dependence of the spectral density FWHM.

temperature with no size changes leads to the Gaussian line shape corresponding to *strong* quasi-2D exciton-phonon coupling. This reflects the enhancement of exciton-phonon coupling in small enough QD's with increasing temperature. Such a behavior of the exciton absorption line shape is well known for bulk excitons where the strength of exciton-phonon coupling is determined by the material.<sup>12</sup> In QW heterostructures, the exciton-phonon coupling strength is governed by the typical size of the quasi-2D exciton localization area which may be controlled technologically, either by a proper choice of the substrate and deposit<sup>1</sup> or by doping with impurities such as nitrogen.<sup>2</sup>

The effects just described will be pronounced in QD's of small enough lateral size where the longitudinal relaxation of excitonic states via inelastic exciton-phonon scattering (population decay) is suppressed due to large exciton level spacing. For 1-ML-thick QD's, this is formulated as  $\hbar\omega_{q_{\parallel LA}} < \Delta E$ , where  $\Delta E \approx \hbar^2/M\xi^2$  is typical level spacing of the quasi-2D exciton parabolically confined in the lateral plane and  $M$  is the exciton effective mass. Since, according to Eq. (9), the maximal phonon momentum is restricted by  $\bar{q}_{\parallel} \approx \sqrt{2}/\xi$ , the ratio  $\hbar\omega_{q_{\parallel LA}}/\Delta E < Mu_{LA}R/2\sqrt{\ln 2}\hbar$  which for GaAs QD's becomes  $\hbar\omega_{q_{\parallel LA}}/\Delta E < 0.015 R(\text{nm})$  and is

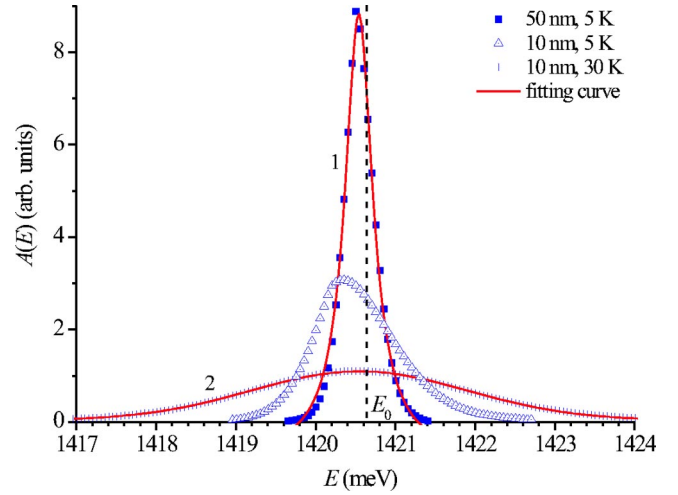


FIG. 4. (Color online) The spectral densities fitted by Lorentzian (1) and Gaussian (2) at the large and small QD size, respectively.

rather small at  $R \sim 10\text{--}20$  nm. Thus, the asymmetric non-Lorentzian effects of exciton pure dephasing must manifest themselves in optical absorption/emission spectra of a single QD at low temperatures. As a matter of fact, the asymmetric shape of the zero-phonon line, although slightly masked by the Lorentzian from the exciton level population decay, is seen in the experimental single QD emission spectra of Ref. 3 below 30 K.

In conclusion, we have showed the enhancement of exciton-phonon coupling in small quasi-2D QD-like islands caused by the interfacial roughness in QW heterostructures. This entails the essentially non-Lorentzian asymmetric shape of the single QD optical absorption/emission line at low temperatures. The asymmetry increases with decreasing the QD lateral size and temperature. We emphasize that this effect may be controlled technologically in process of growing heterostructures—either by a proper choice of the substrate and deposit or by doping with impurities.

We thank Dr. R. Heitz for useful discussions. I.L.K. thanks Alexander von Humboldt Foundation. The work was financially supported by the Foundation for Basic Research of the National Academy of Sciences of the Republic of Belarus (Grants Nos. F01-176, F02R-047) and by NATO SFP Grant No. 972614.

\*On leave from the A. Ioffe Physical-Technical Institute of the Russian Academy of Sciences.

<sup>1</sup>I.L. Krestnikov, N.N. Ledentsov, A. Hoffmann, and D. Bimberg, *Phys. Status Solidi A* **183**, 207 (2001).

<sup>2</sup>A.M. Mintairov *et al.*, *Phys. Rev. Lett.* **87**, 277401 (2001).

<sup>3</sup>L. Besombes, K. Kheng, L. Marsal, and H. Mariette, *Phys. Rev. B* **63**, 155307 (2001).

<sup>4</sup>E. Deleporte *et al.*, *Physica E (Amsterdam)* **13**, 155 (2002).

<sup>5</sup>K. Oshiro, K. Akai, and M. Matsuura, *Phys. Rev. B* **66**, 153308

(2002).

<sup>6</sup>R. Heitz *et al.*, *Phys. Rev. Lett.* **83**, 4654 (1999).

<sup>7</sup>P. Yu. and M. Cardona, *Fundamentals of Semiconductors* (Springer, Berlin, 2001).

<sup>8</sup>T. Takagahara, *Phys. Rev. B* **31**, 6552 (1985).

<sup>9</sup>G. Mahan, *Many-Particle Physics* (Plenum, New York, 1990).

<sup>10</sup>S. Nomura and T. Kobayashi, *Phys. Rev. B* **45**, 1305 (1992).

<sup>11</sup>T. Takagahara, *Phys. Rev. B* **60**, 2638 (1999).

<sup>12</sup>Y. Toyozawa, *Prog. Theor. Phys.* **20**, 53 (1958); **27**, 89 (1962).